

# Dielectric and Electrooptic Investigations of B Phases of Banana-Shaped Thioesters

M. WIERZEJSKA-ADAMOWICZ<sup>a,\*</sup>, D.M. OSSOWSKA-CHRUŚCIEL<sup>b</sup>, J. CHRUŚCIEL<sup>b</sup>,  
R. DOUALI<sup>c</sup>, CH. LEGRAND<sup>c</sup>, M. MARZEC<sup>a</sup>, A. MIKUŁKO<sup>a</sup>, A. SIKORSKA<sup>b</sup>  
AND S. WRÓBEL<sup>a</sup>

<sup>a</sup>Institute of Physics, Jagiellonian University, Reymonta 4, 30-059 Kraków, Poland

<sup>b</sup>Institute of Chemistry, University of Podlasie, 3-go Maja 54, 08-110 Siedlce, Poland

<sup>c</sup>LEMCEL, ULCO, 50 rue F. Buisson, B.P. 717, 62228 Calais, France

Electrooptic and dielectric measurements were done for B phases of two banana-shaped homologues 1,3-phenylene bis{4-[(4-nonyloxybenzoyl)sulfanyl]benzoate (9OSOR) and 1,3-phenylene bis{4-[(4-dodecyloxybenzoyl)sulfanyl]benzoate (12OSOR)}. Polarizing microscopy allowed to identify B<sub>1</sub> phase for 9OSOR and B<sub>2</sub> phase for 12OSOR on the basis of texture observation. Spontaneous polarization measurements were performed using reversal current method. The current response to applied triangular voltage shows that B<sub>1</sub> phase is a ferroelectric and B<sub>2</sub> phase — antiferroelectric one for which two well separated peaks were observed. Polarization for phase B<sub>1</sub> of 9OSOR is rather small and its temperature dependence is unusual for ferroelectric liquid crystals — it increases with temperature. Spontaneous polarization for B<sub>2</sub> phase of 12OSOR compound is of about 600 nC/cm<sup>2</sup>. Dielectric spectra measured with bias field for B<sub>2</sub> phase of 12OSOR show two well separated relaxation processes. In the low frequency range the relaxation process is connected with fluctuations of ferroelectric domains. The relaxation process in the high frequency range appearing also without bias field is connected with molecular reorientation. The dielectric spectra measured for B<sub>1</sub> phase of 9OSOR with and without bias voltage showed only one dielectric relaxation process connected with molecular reorientation around the short axis.

PACS numbers: 77.84.Nh, 77.84.–s, 78.20.Jq

## 1. Introduction

In 1996 Niori and his co-workers found ferroelectric switching of polar smectic phase for a compound built of banana-shaped achiral molecules [1]. Dipolar ordering was a result of rotational restrictions due to steric interactions between the molecules. Different polar order phenomena and chiral properties of B phases allow one to observe ferro- or antiferroelectric behavior as well as electrooptic switching despite the lack of chirality of the molecules [1, 2].

In 1997 the first conference devoted to these phases took place in Berlin. During this conference different structures of them were named from B<sub>1</sub> to B<sub>7</sub>. For B phases there are three independent order parameters: density modulation, tilt angle and layer polarization. These phases show at least one-dimensional positional order. Rotational restriction of banana-shaped molecules results from the long range order of their transverse axes and in consequence — the dipole moments (Fig. 1a). Ferro- or antiferroelectric switching shows B<sub>2</sub> and B<sub>5</sub> phases and also two-dimensional B<sub>7</sub> phases.

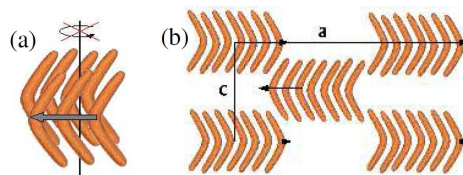


Fig. 1. (a) Rotational restriction around the long molecular axis and (b) alignment of molecules in B<sub>1</sub> phase.

The structure of B<sub>1</sub> phase is shown in Fig. 1b. Side chains of the molecule in one layer overlap the cores of molecules in neighboring layers [3].

The most intensively investigated is B<sub>2</sub> phase in which the molecular long axes are tilted with respect to the layer normal. In order to describe the orientation of banana-shaped molecule in a single smectic layer of B<sub>2</sub> phase three unit vectors are introduced: normal to the layer ( $\mathbf{z}$ ), polarization vector ( $\mathbf{p}$ ) and projection of the  $n$  director on the smectic layer ( $\mathbf{c}$ ). In tilted smectics these vectors can form two coordinate systems:  $(\hat{z}, \hat{c}, \hat{p})$  or  $(\hat{c}, \hat{z}, \hat{p})$  — right- or left-handed, respectively. Smectic structures [4] built of them bear opposite chiralities (Fig. 2).

\* corresponding author; e-mail: marta.wierzejska@uj.edu.pl

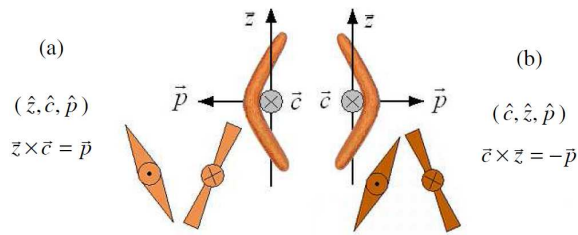


Fig. 2. Coordinate systems and structures built on them.

These chiral layers can be arranged in different ways. The  $B_2$  phase can have four possible structures (Fig. 3) from the left: synclinic — antiferroelectric, anticlinic — antiferroelectric (this phase structure most probably occurs for 12OSOR), synclinic — ferroelectric and anticlinic — ferroelectric [5]. Different types of  $B_2$  phases can be distinguished by using complimentary methods: texture observation, electrooptic response and X-ray diffraction.

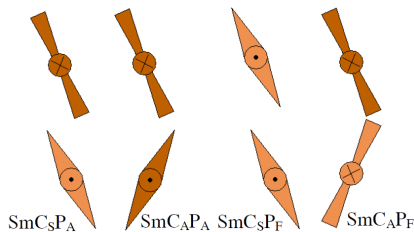


Fig. 3. Theoretically predicted structures of  $B_2$  phase.

The aim of this paper was to investigate electrooptic and dielectric properties of  $B$  phases of two homologues — 9OSOR and 12OSOR.

## 2. Experimental

The core of  $n$ OSOR molecule consists of five phenyl rings interconnected by either ester or thiobenzoate groups as illustrated in Fig. 4 [6]. An important role in smectic  $B_2$  is played by two  $OC_nH_{2n+1}$  alkoxy end chains.  $n$ OSOR molecules are polar, having effective dipole moment ( $\mathbf{p}$ ) along the symmetry axis.

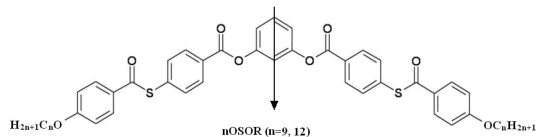


Fig. 4. Molecular structure of  $n$ OSOR compounds.

9OSOR compound shows  $B_1$  phase showing some polarization whereas 12OSOR exhibits antiferroelectric  $B_2$  phase.

Thermal properties of 9OSOR and 12OSOR have been studied by Pyris1 DSC scanning calorimeter. Texture observation and studies of electrooptic switching between

the planar and homeotropic textures for 12OSOR were done at LEMCEL using Olympus Polarizing Microscope BX60 and LINCAM temperature controller. Texture photos of 9OSOR were done in the Institute of Physics of the Jagiellonian University using Nikon Eclipse Polarizing Microscope LV100POL and INSTEC temperature controller.

Spontaneous polarization measurements were carried out — by means of reversal current method (RCM) — using  $1.7 \mu\text{m}$  (for 9OSOR) and  $3.2 \mu\text{m}$  (for 12OSOR) ITO cells. The experimental setup consists of Agilent 3310A wave form generator, FLC electronics amplifier F20ADI and digital scope Agilent DSO6102A and a computer set.

Dielectric measurements were done using dielectric spectrometer based on Agilent 4294A impedance analyzer controlled by PC. Substances — being in isotropic phase — were introduced into Hg —  $5 \mu\text{m}$  gold cells due to capillary effect. The dielectric spectra were acquired in the frequency range from 40 Hz to 25 MHz. Bias field was used to align biaxial  $B_2$  phase so that the polar director  $\mathbf{p}$  is perpendicular to the electrodes. The  $B_2$  is a biaxial phase having the dielectric permittivity tensor of the form

$$\hat{\varepsilon}^*(\nu) = \begin{pmatrix} \varepsilon_{\perp 1}^*(\nu) & 0 & 0 \\ 0 & \varepsilon_{\perp 2}^*(\nu) & 0 \\ 0 & 0 & \varepsilon_{\parallel}^*(\nu) \end{pmatrix}.$$

In this study it was possible to measure two principal components of this tensor, namely  $\varepsilon_{\perp 1}^*(\nu)$  and  $\varepsilon_{\perp 2}^*(\nu)$ .

## 3. Experimental results

### 3.1. Phase diagrams and textures of $B$ phases

Phase diagram of 9OSOR compound show that during heating apart from  $B_1$  phase there are four more phases: probably glassy phase, crystal, a phase that is not identified yet (X) and the isotropic phase. The  $B_1$  phase is enantiotropic one and shows up during cooling in the temperature range of 40 degrees.

- Heating: Cr  $103.4^\circ\text{C}$   $\rightarrow$  X  $112.5^\circ\text{C}$   
 $\rightarrow$   $B_1$   $123^\circ\text{C}$   $\rightarrow$  I
- Cooling: I  $123.4^\circ\text{C}$   $\rightarrow$   $B_1$   $82.6^\circ\text{C}$   $\rightarrow$  Cr

The texture of  $B_1$  phase obtained during cooling is presented in Fig. 5a and b without and with bias field of  $25 \text{ V}_{\text{p-p}}/\mu\text{m}$ , respectively. There is a black line indicating the border line of the electrodes (Fig. 5b). After applying electric field an electrooptic switching is not observed for this phase. Figure 1b illustrates the structure of  $B_1$  phase. As was said above, side chains of the molecule overlap the cores of molecules in neighboring layers and there is a compensation of macroscopic polarization.

Phase diagram for 12OSOR compound shows four phases during the first heating run. Texture observations using polarization microscope allowed us to identify them as Cr1, Cr2,  $B_2$  phase and isotropic phase. During the

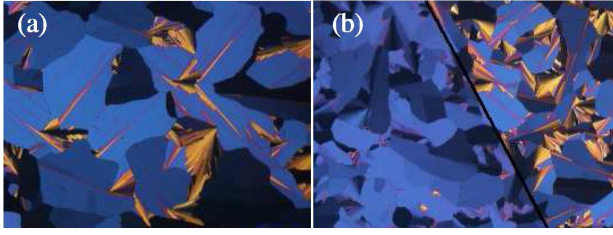


Fig. 5.  $B_1$  phase texture of 9OSOR at  $T = 105^\circ\text{C}$ : (a)  $U = 0 \text{ V}_{\text{p-p}}/\mu\text{m}$  and (b)  $U = 25 \text{ V}_{\text{p-p}}/\mu\text{m}$ .

second heating run only one crystalline phase was observed. The  $B_2$  phase is enantiotropic one and shows up during cooling in the temperature range of 20 degrees.

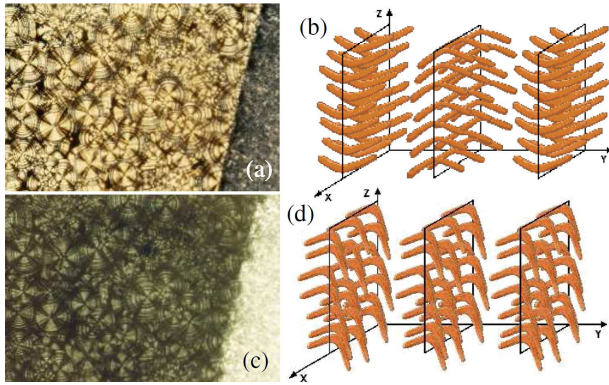


Fig. 6. (a) Planar inhomogeneous texture of  $B_2$  phase in  $T = 116.8^\circ\text{C}$ ,  $U = 0 \text{ V}_{\text{p-p}}/\mu\text{m}$  and (b) alignment of molecules in planar  $B_2$  phase of 12OSOR compound, (c) homeotropic texture of  $B_2$  phase in  $T = 116.8^\circ\text{C}$ ,  $U = 13 \text{ V}_{\text{p-p}}/\mu\text{m}$  and (d) homeotropic alignment of molecules in  $B_2$  phase of 12OSOR compound.

- Heating: Cr2  $88^\circ\text{C} \rightarrow$  Cr1  $107.1^\circ\text{C} \rightarrow$   $B_2$   $113.4^\circ\text{C} \rightarrow$  I.

Polarizing microscopy measurements allowed us to observe on thin layers ( $1.7 \mu\text{m}$ ) a planar inhomogeneous (Fig. 6a) and homeotropic (Fig. 6c) textures of  $B_2$  phase. The homeotropic texture was observed for bias field equal to  $13 \text{ V}_{\text{p-p}}/\mu\text{m}$ . Figures 6b and d present also molecular arrangement of planar and homeotropic textures, respectively.

- Cooling: I  $112.6^\circ\text{C} \rightarrow$   $B_2$   $88.6^\circ\text{C} \rightarrow$  Cr1.

### 3.2. Spontaneous polarization

Usually  $B_1$  phases do not show spontaneous polarization although for 9OSOR compound an apparent polarization is observed (Fig. 7a) [7]. Polarization for phase  $B_1$  is rather small and its temperature dependence is unusual as for ferroelectric liquid crystals — it increases with temperature (Fig. 7b). Measurements were done

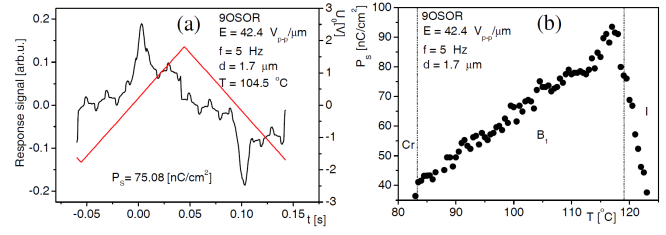


Fig. 7. (a) Triangular driving voltage (right-hand side scale) applied and reversal current spectrum (left-hand side scale) and (b) apparent polarization vs. temperature of ferroelectric  $B_1$  phase in 9OSOR.

using triangular electric field having frequency of 5 Hz and amplitude equal to  $21.2 \text{ V}_{\text{p-p}}/\mu\text{m}$ .

The  $B_2$  phase of 12OSOR compound seems to be antiferroelectric — antiferroelectric ( $\text{SmC}_{\text{A}}\text{P}_{\text{A}}$ ), after applying to the electrodes triangular electric wave, two peaks are observed (Fig. 8a) for the sample. As seen in Fig. 8b, spontaneous polarization is very high — it reaches  $600 \text{ nC}/\text{cm}^2$  [6]. Measurements were done using driving electric field of  $18.8 \text{ V}_{\text{p-p}}/\mu\text{m}$  and signal frequency of 20 Hz.

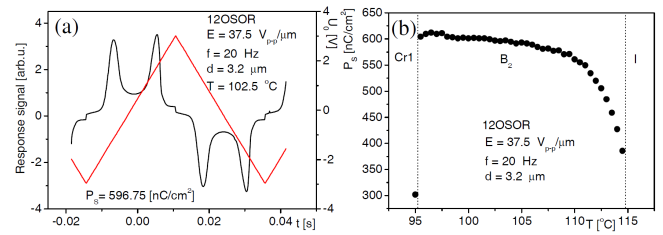


Fig. 8. (a) Triangular driving voltage (right-hand side scale) applied and reversal current spectrum (left-hand side scale) and (b) spontaneous polarization vs. temperature of antiferroelectric  $B_2$  phase in 12OSOR.

### 3.3. Dielectric measurements

Figures 9a and b show 3D graphs of dielectric absorption measured without and with bias voltage equal to 5 V for 9OSOR compound. As seen in both cases, only one relaxation process shows up and is connected with molecule reorientation around the short axes. The activation energy is equal to  $\Delta E = 112 \text{ kJ}/\text{mol}$  with and without bias voltage as well (Figs. 10a and b).

There were some difficulties with choosing the right fitting function for the low frequency part of the spectrum where conductivity contribution to the dielectric loss plays an important role. At low frequencies the dispersion behaves rather unusual — it is linear on the logarithmic scale for the investigated compound. The best fitting function occurred to be a function with extra parameters

$$\varepsilon^*(\nu) = \varepsilon(\infty) + \frac{\varepsilon(0) - \varepsilon(\infty)}{1 + (i2\pi\nu\tau)^{1-\alpha}} - \frac{iA}{\nu^M} + \frac{B}{\nu^N},$$

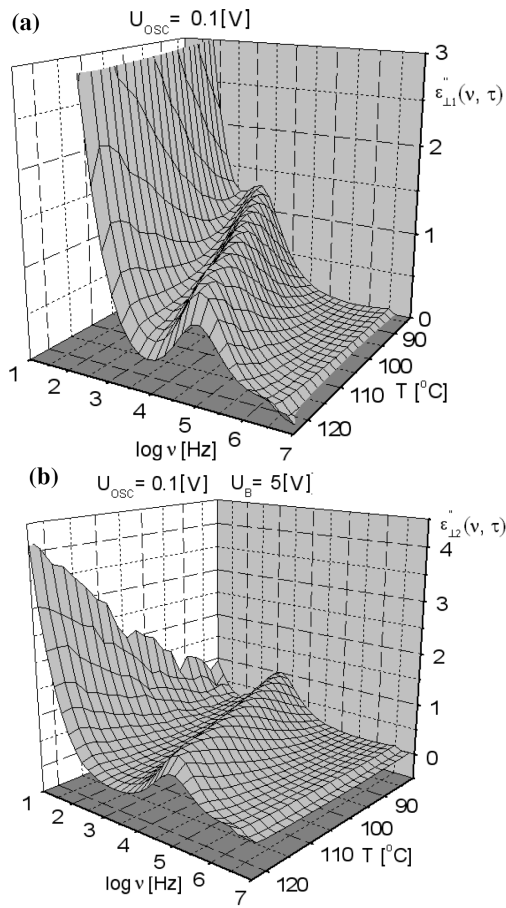


Fig. 9. Dielectric loss vs. frequency for B<sub>1</sub> phase in 9OSOR obtained: (a) without bias voltage and (b) under bias voltage equal to 5 V.

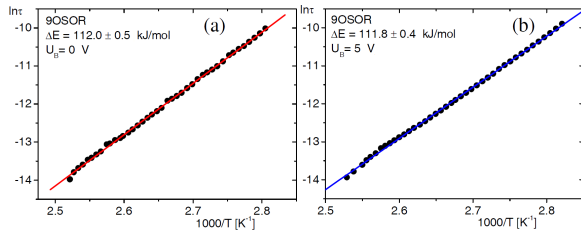


Fig. 10. Arrhenius plot for the dielectric relaxation process for B<sub>1</sub> phase of 9OSOR observed: (a) without bias voltage and (b) with bias voltage.

where  $\varepsilon_0 = 8.854187817 \times 10^{-12}$  F/m,  $\nu$  — frequency,  $\varepsilon(0)$  — static electric permittivity,  $\varepsilon(\infty)$  — boundary electric permittivity at high frequencies,  $\tau$  — relaxation time,  $\sigma$  — conductivity,  $A = \frac{\sigma}{(2\pi)^M}$ ;  $\varepsilon(0)$ ,  $\varepsilon(\infty)$ ,  $\tau$ ,  $A$ ,  $\alpha$ ,  $B$ ,  $M$ ,  $N$  are the fitting parameters. Such a function was used successfully by Kresse et al. [8]. This function is typically used for smectic phases built of banana-shaped molecules. As shown for calamitic liquid crystals one can easily fit normal conductivity term [9].

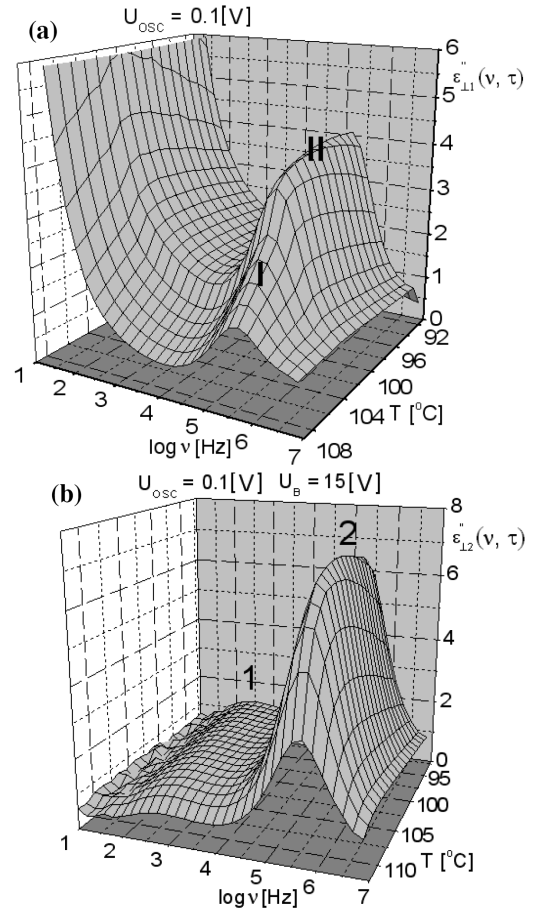


Fig. 11. Dielectric loss vs. frequency for B<sub>2</sub> phase in 12OSOR measured: (a) without bias voltage and (b) under bias voltage equal to 15 V.

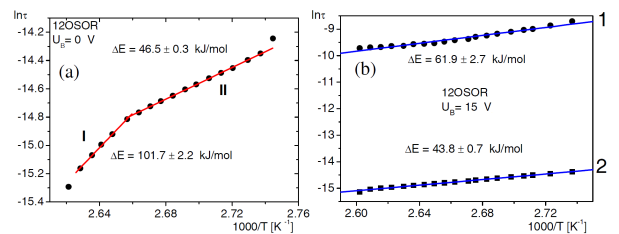


Fig. 12. Arrhenius plot for the dielectric relaxation process for B<sub>2</sub> phase of 12OSOR observed: (a) without bias voltage and (b) with bias voltage.

Figures 11a and b show 3D graphs of absorption acquired without and with bias voltage equal to 15 V for 12OSOR compound. Dielectric spectra measured with bias voltage show two well separated relaxation processes on the contrary to B<sub>1</sub> phase of 9OSOR (Figs. 9a and b). In the low frequency range the relaxation process is connected with fluctuations of ferroelectric domains revealing in homeotropic structure of B<sub>2</sub> phase. The relaxation process in high frequency range appearing also without bias field is connected with reorientation of molecules.



For 12OSOR this process is complex: in the high temperature range of B<sub>2</sub> phase it is connected with reorientation of molecules around the short axis (process **I**), whereas in the low temperature range — around the long axis (process **II**) [10]. Activation energy of the process connected with fluctuations of domains is equal to  $\Delta E = 62$  kJ/mol with bias voltage (Fig. 12b), whereas for the process connected with reorientation around the long molecular axis it is of about 45 kJ/mol with and without bias voltage (Figs. 12a and b). Activation energy for reorientation around the short axis process — observed in the pretransition region — is equal to  $\Delta E = 102$  kJ/mol (Fig. 12a).

#### 4. Conclusions

- Our studies show that B<sub>1</sub> phase of 9OSOR does not exhibit any low frequency dielectric relaxation process of collective nature.
- On the contrary, 12OSOR with even number of carbon atoms in alkoxy side chains exhibits antiferroelectric SmC<sub>A</sub>P<sub>A</sub> phase showing both collective and molecular dielectric relaxation processes. Two principal components ( $\varepsilon_{\perp 1}^*(\nu)$  and  $\varepsilon_{\perp 2}^*(\nu)$ ) of the dielectric permittivity tensor show qualitatively different dielectric relaxation spectra for this biaxial phase.

#### References

- [1] T. Noiri, T. Sekine, J. Watanabe, T. Furukawa, H. Takezoe, *J. Mater. Chem.* **6**, 1231 (1996).
- [2] T. Sekine, Y. Takanishi, T. Noiri, J. Watanabe, H. Takezoe, *Jpn. J. Appl. Phys.* **36**, L1201 (1997).
- [3] J. Ortega, M.R. de la Fuente, J. Etxebarria, C.L. Folcia, S. Díez, J.A. Gallastegui, N. Gimeno, M.B. Ros, M.A. Pérez-Jubindo, *Phys. Rev. E* **69**, 011703 (2004).
- [4] N. Vaupotič, *Ferroelectrics* **334**, 151 (2006).
- [5] M.B. Ros, J.L. Serrano, M.R. de la Fuente, C.L. Folcia, *J. Mater. Chem.* **15**, 5093 (2005).
- [6] J.C. Rouillon, J.P. Marcerou, M. Laguerre, H.T. Nguyen, M.F. Achard, *J. Mater. Chem.* **11**, 2946 (2001).
- [7] D.M. Ossowska-Chruściel, K. Kudłacz, A. Sikorska, J. Chruściel, M. Marzec, A. Mikułko, S. Wróbel, R. Douali, Ch. Legrand, *Phase Transit.* **80**, 781 (2007).
- [8] Z. Vakhovskaya, W. Weissflog, R. Friedemann, H. Kresse, *Phase Transit.* **80**, 705 (2007).
- [9] A. Mikułko, M. Fraś, M. Marzec, S. Wróbel, M.D. Ossowska-Chruściel, J. Chruściel, *Acta Phys. Pol. A* **113**, 1155 (2008).
- [10] D.M. Ossowska-Chruściel, M. Wierzejska-Adamowicz, M. Marzec, A. Mikułko, R. Douali, Ch. Legrand, J. Chruściel, A. Sikorska, S. Wróbel, *Phase Transit.* **82**, 889 (2009).